



ISSN 0975-413X
CODEN (USA): PCHHAX

Der Pharma Chemica, 2016, 8(2):365-374
(<http://derpharmachemica.com/archive.html>)

***In silico* design of new MPS1 inhibitors via a validated structure-based virtual screening approach**

Mohammad A. Ghattas, Mohammad Al Sorkhy and Noor Atatreh*

College of Pharmacy, Al Ain University of Science and Technology, Al Ain, UAE

ABSTRACT

Cell cycle is a highly coordinated and well conserved process and abrogation in the cell cycle are a hallmark of many types of cancer, thus, it has been under the spotlight as a target of anti-cancer therapeutics for decades. A wide range of tumor-associated mutations have been linked to abnormal regulation of protein kinases. MPS1 protein family is dual-specific protein kinases among several that are heavily involved in cell cycle regulation, abrogation in MPS1 have been linked to many types of cancer. Targeting MPS1 by small molecule inhibitors has attracted many researchers due to their high involvement in cancer progression. However, despite numerous trials, MPS1 inhibitors failed to reach clinical trials. In this work, we studied the protein-ligand interactions via an automated approach. At least one interaction with the MPS1 hinge region was found to be key for protein ligand binding and was used as basis for creating pharmacophoric docking constraints. Several docking protocols, e.g. standard and constrained docking protocols, were examined for their MPS1 virtual screens' enrichment. It was found that constrained docking followed by refinement step had the superiority over other examined docking protocols. Accordingly, virtual screening for druglike library was pursued. Several hits were nominated for in vitro testing in the future as they showed convenient binding modes with the MPS1 pocket, in particular, satisfying the key interactions with the MPS1 hinge region. The knowledge-based drug design strategy explored and conducted here can potentially inform new MPS1 inhibitors.

Key words: MPS1, drug design, virtual screening, inhibitors, constrained docking.

Abbreviations: VS, virtual screening; PLIF, protein-ligand interaction fingerprint; EF, enrichment factor; HBD, hydrogen bond donor; HBA; hydrogen bond acceptor.

INTRODUCTION

Cell cycle regulation is highly controlled process that plays a critical role in all cell fate decisions, protein kinases are major regulators of such important process [1]. Aside from the cyclin-dependent kinases (CDKs), the traditional cell cycle regulators, many kinases are emerging as key mitotic regulators such as Polo, Bub and MPS1 [2]. The MPS1 (monopolar spindle) family is newly discovered protein kinases and they are under the microscope for potential drug targets due to their unique mitotic regulation role [2].

MPS1 protein kinases are predominantly found in Eukaryotas. This family of protein kinases is among many families known to regulate a number of steps of mitosis. Several MPS1 kinase functions have been heavily studied particularly those involve activities at the kinetochore in both the chromosome attachment and the spindle checkpoint; they have been also found to function at centrosomes [2]. Away from mitosis, MPS1 kinases have been found to have key function in development, cytokinesis, and many signaling pathways. MPS1 abrogation in many

types of cancers has put them in the spotlight for anticancer drug design. Like other cell-cycle regulators, Mps1 levels are abrogated in a variety of human cancers [2].

Mps1 mRNA levels are found to be upregulated in many different human tumors, including thyroid papillary carcinoma, breast cancer, gastric cancer tissue, and lung cancers [3-5], moreover, high levels of Mps1 has been found in higher grades of breast cancers [6]. On the contrary, Mps1 mRNA is significantly depleted or absent in resting cells and in tissues with a low proliferation rate [7]. Therefore, the relation between elevated Mps1 levels and cell proliferation as well as with tumor aggressiveness is clearly undeniable. This clear correlation has put MPS1 in the spotlight as anti-cancer target.

The emergence of MPS1 as a novel drug target for cancer therapy, has paved the road for many research groups to start exploring the possibility of targeting them. The first small inhibitor of Mps1 was Cincreasin which has been found to not to be very potent with 50% inhibitory concentration (IC₅₀) = 700 μM [8]. After that, many structurally distinct inhibitors have been studied and tested, with a wide range of potency (IC₅₀) ranging from 8 to 700nM. None of these inhibitors have made it yet to the clinical studies [9, 10] as the lack of excellent selectivity profile was a major obstacle faced these inhibitors. More recently, two small molecule inhibitors have showed an excellent selectivity profile with an IC₅₀ below 10nM, BAY 1161909 and BAY 1217389 have achieved moderate efficacy in vivo tumor xenograft studies [11].

It is clearly critical to keep exploring new small molecule inhibitors that specifically target MPS1 until reliable highly specific molecules pass the clinical studies. Herein, we optimize and analyze MPS1-ligand interactions to work out which is key for ligand binding. Consequently we validate and conduct structure-based virtual screening for the discovery of new potential MPS1 inhibitors.

MATERIALS AND METHODS

Analysis of MPS1-ligand complexes

A set of 15 MPS1-ligand complexes was obtained from the Protein Data Bank [12]. All 15 crystal structures underwent a visual and automatic check via the protein preparation wizard [13]. Afterward, automated protein-ligand analysis was carried out on the whole set of MPS1-ligand complexes using the MOE software package [14]. A protein-ligand interaction fingerprint (PLIF) [13] was generated for each complex. PLIF methodology is discussed elsewhere [15]. Minimum score threshold for hydrogen bonding was set as 1%; and 5% for ionic interaction. Interactions scored less than the identified thresholds not considered in the final PLIF. The obtained PLIF graph shows the interaction occupancy of each residue in the MPS1 active site that is involved in interaction with any of the MPS1 inhibitors. This interaction occupancy is defined as the percentage of ligands interacting with the side chain or the main chain of a given amino acid.

Preparation of Test sets for seeding experiments

A test set was prepared for conducting virtual screening seeding experiments against the ATP binding site of the MPS1 structure. The test set was composed of two main types of ligands: firstly, known MPS1 inhibitors (15 ligands) which were found co-crystallized with MPS1 in the PDB. Secondly, decoy ligands (985 ligands) were selected randomly from a commercial database (TimTec [16]) in order to act as inactive ligands. Both types of ligands, known inhibitors and decoys, were processed via the *wash* module in MOE [13] in order to add missing hydrogens and to assign their ionization state at pH 7. Partial charges were given for each ligand which was then energy minimized via the MMFF94x forcefield [17-23].

Protein preparation for seeding experiments and VS

The MPS1 crystal structure was obtained from the protein data bank (PDB ID: 3HMO). The structure was checked and repaired for any missing atom, residue or loop via the protein preparation wizard in MOE [14]. Using the MOE *3D protonate* module [13], hydrogen atoms were added to the MPS1 enzyme structure and partial charges were assigned on each atom based on the MMFF94 forcefield [18-22]. All water molecules were removed prior protein preparation. The docking site was identified via the coordinates of the co-crystallized ligand.

Docking protocols used in VS validation

A hinge region pharmacophore was designed before docking using the MOE *Pharmacophore Elucidation* module [13] for use in the constrained docking protocol. Two pharmacophore points were created according to the

coordinates of the γ -lactam oxygen and nitrogen atoms that are hydrogen bound to the backbone amide of the hinge region. The first pharmacophore point was set as essential and it only accepts hydrogen bond acceptor (HBA) whilst the second point was set as optional and it only accepts hydrogen bond donor (HBD). Then, the prepared test set was docked into the ATP binding site on the MPS1 protein using the MOE-Dock program. Triangle Match and Pharmacophore [13] were employed as placement methods in the standard and constrained docking protocols, respectively. The London dG function was employed to score generated poses of each docked ligands. A brief description of the both docking algorithms and the scoring function is discussed elsewhere [13, 24]. Docking output finally involved the only top ranked pose of each docked ligands which sorted according to their docking scores.

Pharmacophoric constraints to the two previously defined pharmacophoric points were applied in the constrained docking protocol. Only poses that met at least the essential pharmacophoric feature were considered for scoring. Where applicable, the best pose of each ligand generated from constrained docking was refined via the MMFF94x forcefield [18-23] inside the MPS1 ATP binding site and then scored via GVBI/WSA scoring function. Consensus scoring that involved both the GVBI/WSA and the London dG scoring functions was employed to rank the final list of ligands. Known inhibitors appeared in the top 1%, 3%, 5% and 10% of the docked ligand library were counted so that to calculate the enrichment factor (EF). EF for the top $n\%$ was calculated using the following equation.

$$EF_{top\ n\%} = \frac{\text{number of inhibitors ranked in the top } n\% \text{ of screened library}}{\text{total number of known inhibitors}} \times 100\%$$

Ligand library preparation for VS

A ligand library was obtained from the National Cancer Institute/USA [25] and Timtec Company [16]. Two filtration rules for druglike characteristics were applied: the Veber's rules [26] and the Lipinski's rule of five [27]. Such rules involve: molecular weight ≤ 500 , hydrogen bond donor (HBD) ≤ 5 , hydrogen bond acceptor (HBA) ≤ 10 , $\log P \leq 5$, polar surface area (PSA) ≤ 140 and rotatable bonds ≤ 10 . Ligands were assigned a protonation state based on the Wash module in MOE [13, 14] and then atoms were given partial charges based on the MMFF94x force field [18-23].

Virtual screening protocol

The constrained/refined docking protocol was employed here to screen the drug-ligand like library against the previously prepared MPS1 active site. Thus, the pharmacophoric constraints were applied during the docking process via the *Pharmacophore docking algorithm* [13]. London dG [13] was employed as a scoring function to score and rank poses generated from the placement stage; only the top ranked pose of each docked ligand was considered in the output list.

The top 10% of the docked library was refined via the MMFF94x force field [18-23] and were then assigned binding energies by the GBVI/WSA dG scoring function [13]. Consensus scoring, that involved the sum of ranks from GVBI/WSA and London dG scoring, was employed to rank the final list of ligands. Using the MACCS algorithm [28], top 2000 ligands of the refined list were clustered and visually inspected. The clustering main parameters, similarity and overlapping, were set to 60. Ligands from various chemical scaffolds that showed pleasant binding modes and convenient pocket filling were selected for the final hit list.

As for the reference ligand docking and scoring, we used the active conformation the co-crystallized ligand with MPS1 (PDB: 3HMO). The 3HMO ligand, staurosporine, was constrained docked and refined inside the ATP binding site of MPS1 and was then scored based on the GBVI/WSA dG scoring function.

RESULTS AND DISCUSSION

Analysis of ligand-MPS1 complexes

To attain better understanding for the key interactions necessary for ligand binding to MPS1, the ATP binding site should be assessed along with the co-crystallized inhibitors [29]. We performed automated protein-ligand interaction analysis on 15 MPS1-ligand complexes which was followed by visual analysis. This automated analysis was conducted by producing protein-ligand interaction fingerprints (PLIF) for each MPS1-inhibitor co-crystallized complex. Each residue in the MPS1 active site has scores for its side chain and backbone amide interactions. As shown in Figure 1, seven residues mainly appear to contribute to the stabilization of MPS1 inhibitors inside the ATP

binding site; for clarity, only the amino acids involved in two or more interactions are shown in the PLIF graph (Figure 1).

The PLIF profile illustrates the importance of the conserved hinge region in the ATP binding site for stabilising the MPS1 inhibitors in the catalytic pocket: almost all tested complexes appear to be involved in at least one hydrogen bonding with one of the hinge region residues, particularly Gly605 which had an occupancy of 87% (Figure 1) and/or Glu607 which had an occupancy of 47%. Lys553 was also capable of making high number of ligand interactions, with an occupancy of 53% (Figure 1). Actually, only one MPS1 inhibitor failed to interact with the backbone amide of the both hinge region residues. As for the surface contact, Ile531 was able to form such interactions with 93 % of the MPS1 inhibitors. Other three residues, Ile607, Asp608 and Ile663 were involved in a less number of interactions with the examined ligands, with occupancies ranging between 13 % and 27%. From visual inspection of the MPS1 crystal complexes, all co-crystallized ligands appear to have a HBA and, to less extent, HBD on their structures that make the crucial hydrogen bonding observed in our PLIF study.

Validation of virtual screening

The effect of various docking factors and protocols on virtual screening can be evaluated by conducting a series of docking experiments, called seeding, against the MPS1 enzyme. Seeding experiments are performed via mixing known inhibitors with presumed inactive ligands and then dock the newly formed test set into the target active site [29]. This should be done for two times, in the presence and absence of that examined factor. Afterwards, enrichment factor (EF) of each screen is calculated via counting the known inhibitors that have been retrieved in the top-ranked list of docked compounds [29]. EF values are then compared so the importance of that particular factor on the virtual screening can be evaluated.

Kinases were studied by Perola [30] and they were found to have a conserved loop that is called “hinge” region which is regularly involved in one or two hydrogen bonding with the kinase inhibitor. Additionally, it was observed by the same scientist [30] that using constrained docking to force such an interaction with the hinge region is favourable for virtual screening. As mentioned previously, in the case of MPS1, the Gly605 and to a lesser extent Glu603 are the main residues in the hinge region that are commonly observed interacting with the MPS1 inhibitors. Thus, it was important to check if Perola’s observation can be generalized to MPS1. Accordingly, we created a two-point pharmacophore (

Figure 2) based on the co-crystallized MPS1 inhibitor that involves an essential feature (HBA to interact with Gly605) and an optional feature (HBD to interact with Glu603).

Three docking protocols were evaluated here: (1) a *standard* docking protocol, where ligands are placed by the Triangle Match algorithm and generated poses are scored via London dG; (2) a *constrained* docking protocol, where ligands were placed by the Pharmacophore algorithm and generated poses were then scored via London dG; and (3) a *constrained/refined* docking protocol, where ligands were placed by the Pharmacophore algorithm and generated poses were scored via London dG and then refined via MMFF94x forcefield. The refined poses were rescored via the GBVI/WSA dG scoring function and the final ligand output was ranked via consensus scoring using both London dG and GBVI/WSA dG. In the *constrained* and *constrained/refined* docking protocols, the previously created two-point pharmacophore was used to guide the placement of the ligand atoms.

Enrichment factors were calculated for the three docking protocols employed during the ligand screening against the MPS1 active site (

Table 1). Firstly, for screening with the *standard* protocol, we find that the $EF_{top3\%}$ value was equal to 20. Secondly, the *constrained* protocol was able to retrieve one third of the known inhibitors in the top 3%, ($EF_{top3\%} = 33$), which is greater than the *standard* docking by 32 %. Thirdly, the *constrained/refined* protocol was able to achieve as high EF value as 60, which is almost two times greater than the *constrained* protocol and even three times greater than the *standard* protocol. Looking at their enrichment profile, it can be concluded that the *constrained/refined* protocol had clear superiority over the other two protocols, confirming the importance of the MPS inhibitors interaction with the hinge region and emphasizing the significance of having a post-docking processing to filter out top-ranked ligands with unreasonable binding mode. Constraining docking to previously identified key interactions also showed

superiority over standard docking in the protein tyrosine phosphatases [24] and enoyl acyl carrier protein reductases [31] virtual screens; by enhancing their enrichment and docking accuracy.

Structure-based virtual screening

The previously prepared drug-like ligand library was docked into the ATP binding site of MPS1. A scheme representing our virtual screening work flow is shown in

Figure 4. The workflow started with filtering the initial ligand library as per the common druglike rules, decreasing the size of the ligand library from 852,929 ligands to 632,546 ligands. In the other hand, the MPS1 protein structure was checked and prepared. Afterwards, the druglike ligand library was docked into the ATP binding site on the MPS1 structure. Throughout docking, the previously prepared pharmacophoric constraint was employed to ensure key interactions with the hinge region of the ATP binding site will take place. Only 539,514 ligands were able to satisfy the pharmacophoric features and appeared in the docked ligand list produced by constrained docking. The top 10 % of this list was refined inside the MPS1 pocket so that ligand-protein interactions can be optimized and clashes with the surrounding residues can be eliminated. The top 2000 ligands were clustered into different chemical classes and were visually inspected for their pocket filling and binding mode suitability. Accordingly, 50 compounds belong to different structural clusters were nominated for future *in vitro* testing.

Table 2 shows selected examples from the final hit list along with their predicted binding energies, consensus rank and cluster number. Interestingly, most of the selected compounds had better docking scores than the reference ligand, staurosporine, and contained many of the key structural features that are important for MPS1 binding. As the GBVI/WSA dG function considers more terms in its final predicted scores than London dG, mainly scores from the former function are considered within the following text. The binding energies of the selected hits indicate for favorable binding with MPS1. The four shown hits in Table 2 were able to obtain GBVI/WSA dG scores within the range of -7.0 and -7.3 kcal/mol, which is even lower than the reference ligand (-6.2 kcal/mol).

The binding modes of the four hits are shown in

Figure 5 and Figure 6 where all ligands can be observed to form at least one interaction with hinge region backbone amide. As shown in

Figure 5A, compound ST025178 was able to form a hydrogen bonding with Lys553 via its ether oxygen and an ionic interaction with Lys649 via its carboxylate group. Additionally, ST025178 was involved in multiple van der Waals interactions with the surrounding residues, in particular, with the key residue Ile531. As shown in

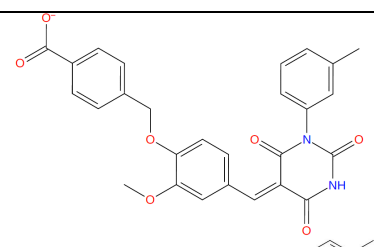
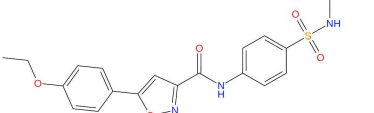
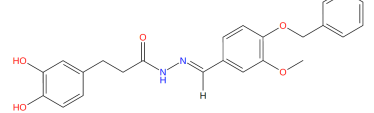
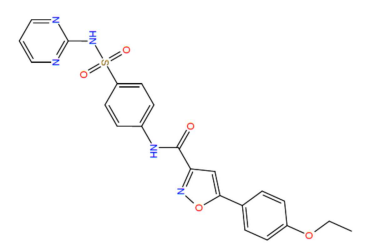
Figure 5B, ST45224452 appears to be nicely filling the active site in addition to forming key hydrogen bonding with the Gly605 backbone amide via its amide carbonyl and another hydrogen bonding with the Lys553 side chain via its ether oxygen.

The binding mode of compound ST50710122 is shown in Figure 6A where the key interaction with the MPS1 hinge region is seen between the ligand ether oxygen and the Gly605 backbone amide. Interestingly, this compound appears to be involved in two electrostatic interactions with the Lys553 protonated amine. The first interaction is hydrogen bonding that was formed by the ligand amide carbonyl and the second interaction is cation- π interaction that was made by the terminal aromatic ring of compound ST50710122. The latter interaction was also seen in the binding mode of compound ST45225022, as shown in Figure 6B. Additionally, ST45225022 was capable of forming two hydrogen bonding interactions with the hinge region backbone amides. All in all, the validated VS approach used in this work suggested a list of interesting hits that could act as inhibitors for MPS1 in the future.

Table 1. Enrichment factors obtained for three different docking protocols at different top ranked library percentages

Top ranked library %	Standard	Constrained	Constrained/Refined
Top 3%	20.0	33.3	60.0
Top 5%	26.6	66.7	66.7
Top 10%	40.0	80.0	80.0

Table 2. The GBVI/WSA dG and London dG scores of the selected best hits obtained from the receptor-based virtual screening against MPS1, along with their consensus rank and cluster number

Compound ID	2D structure	London dG	GBVI/WSA dG scores (kcal/mol)	Rank by Consensus	Cluster
ST025178		-15.38	-7.23	17	1
ST45224452		-15.93	-7.00	25	25
ST50710122		-15.44	-7.10	28	28
ST45225022		-15.19	-7.28	29	5
staurosporine	reference co-crystallized ligand	-12.8	-6.19	467.5	-

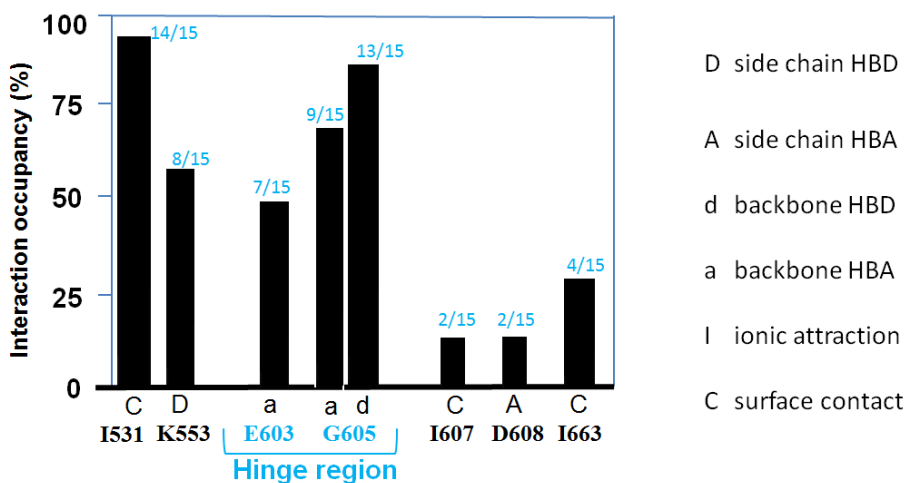


Figure 1. A graph shows PLIFs of 15 ligand-MPS1 complexes assessed in this study. For clarity, only amino acids involved in the greatest number of interactions are shown

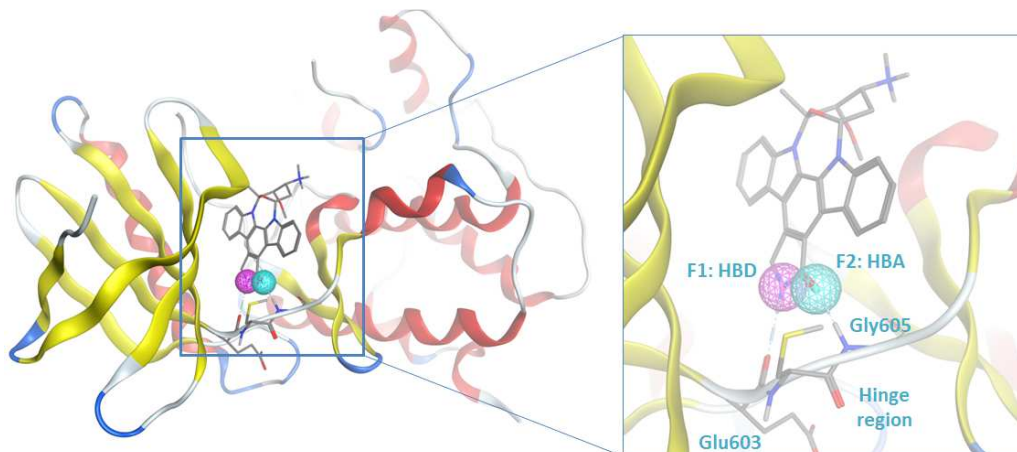


Figure 2. The MPS1 3D structure along with the two-point Pharmacophore that was created based on the co-crystallized ligand inside the ATP binding site

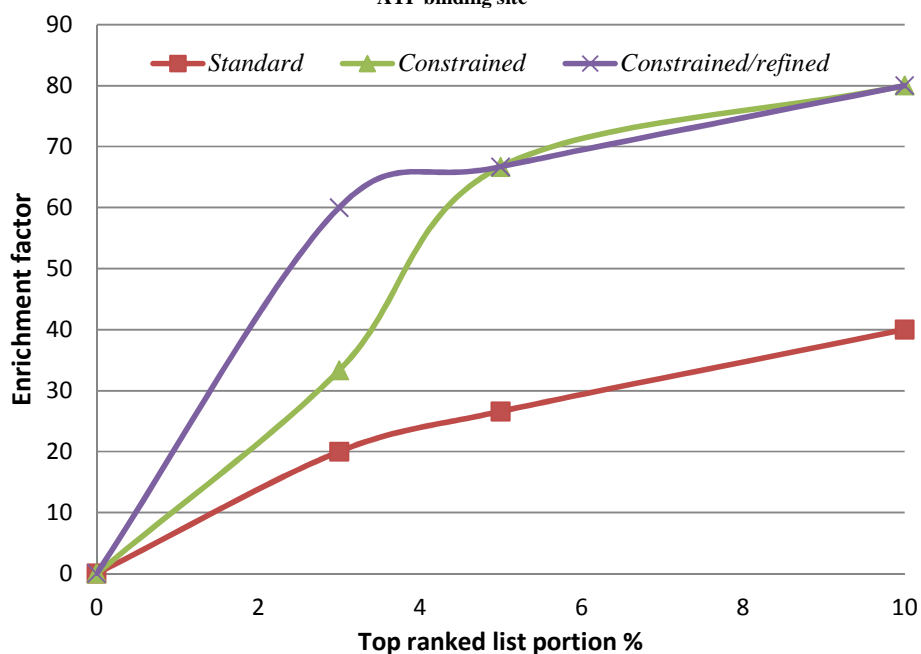


Figure 3. A graph shows the enrichment profiles at different portions of the top-ranked ligand list resulting from multiple MPS1 screens using the three examined docking protocols

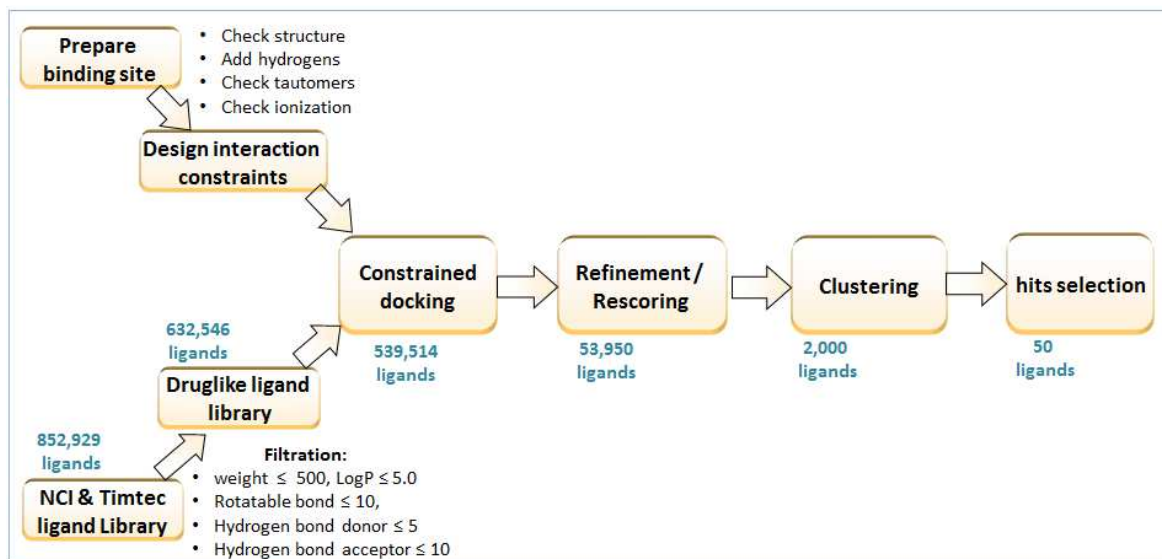


Figure 4. A scheme shows the virtual screening workflow employed against MPS1 using a druglike ligand library

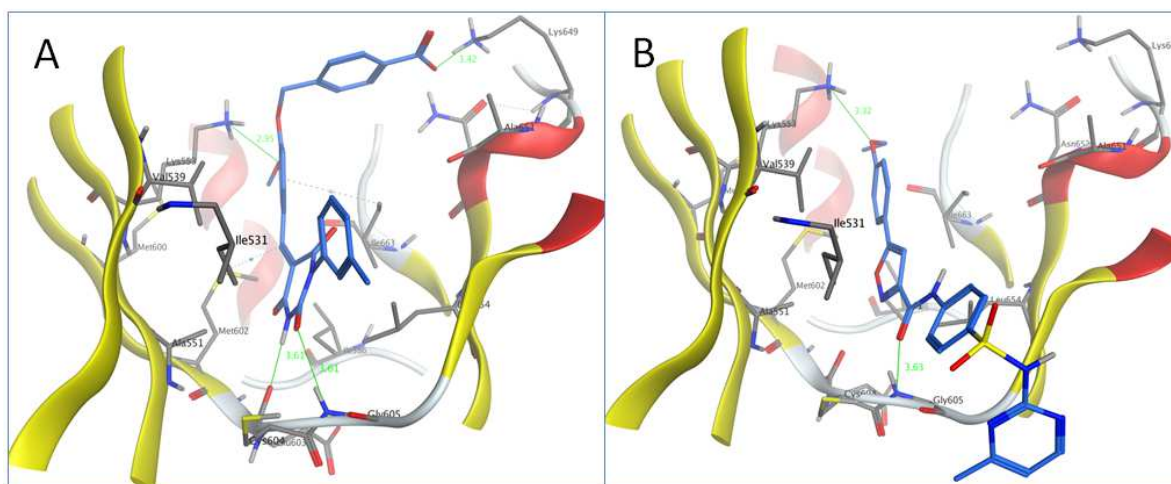


Figure 5. Predicted binding modes of ST025178 (A) and ST45224452 (B) with the ATP pocket of the MPS1 enzyme. Some of the protein structure is not shown for clarity

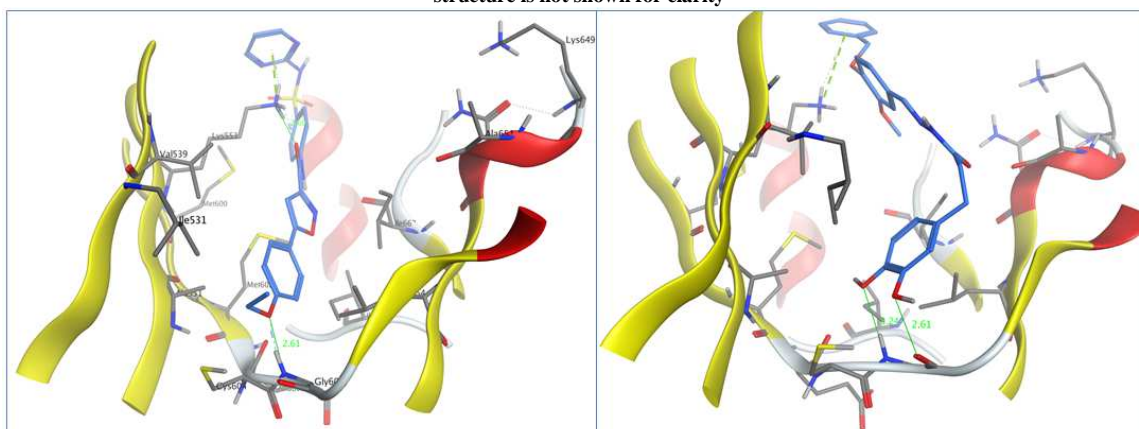


Figure 6. Predicted binding modes of ST45225022 (A) and ST50710122 (B) with the ATP pocket of the MPS1 enzyme. Some of the protein structure is not shown for clarity

CONCLUSION

Analysis of protein-ligand interactions for a set of 15 MPS1-ligand complexes revealed that almost all known inhibitors were involved in at least one interaction with the MPS1 hinge region, mainly the Gly605 backbone amide. Accordingly, a pharmacophoric constraint was created to force these interactions with the hinge region and once applied throughout docking; it enhanced the enrichment of the MPS1 screen in a clear manner. Following the constrained docking with a refinement step was clearly able to even further enhance the MPS1 screening enrichment. Applying this validated protocol in screening a large drug-like library against the ATP binding site of MPS1 produced a number of interesting hits that could act as potential anticancer agent in the future. These hits have even lower binding energies than the reference inhibitor staurosporine and have many of the required features to inhibit the MPS1 enzyme.

Acknowledgements

This work was funded by a grant from the Deanship of Scientific Research and Graduate Studies at Al Ain University of Science and Technology, Al Ain, UAE.

REFERENCES

- [1] T Hunter. *Cell*.**2000**, *100*, 113-127.
- [2] X Liu, M Winey. *Annu. Rev. Biochem.***2012**, *81*, 561-585.
- [3] M T Landi, T Dracheva, M Rotunno, J D Figueroa, H Liu, A Dasgupta, F E Mann, J Fukuoka, M Hames, A W Bergen, S E Murphy, P Yang, A C Pesatori, D Consonni, P A Bertazzi, S Wacholder, J H Shih, N E Caporaso, J Jen. *PLoS ONE*.**2008**, *3*, e1651.
- [4] G B Mills, R Schmandt, M McGill, A Amendola, M Hill, K Jacobs, C May, A M Rodricks, S Campbell, D Hogg. *J. Biol. Chem.***1992**, *267*, 16000-16006.
- [5] G Salvatore, T C Nappi, P Salerno, Y Jiang, C Garbi, C Ugolini, P Miccoli, F Basolo, M D Castellone, A M Cirafici, R M Melillo, A Fusco, M L Bittner, M Santoro. *Cancer Res.* **2007**, *67*, 10148-10158.
- [6] J Daniel, J Coulter, J H Woo, K Wilsbach, E Gabrielson. *Proc. Natl. Acad. Sci.***2011**, *108*, 5384-5389.
- [7] D Hogg, C Guidos, D Bailey, A Amendola, T Groves, J Davidson, R Schmandt, G Mills. *Oncogene*.**1994**, *9*, 89-96.
- [8] R K Dorer, S Zhong, J A Tallarico, W H Wong, T J Mitchison, A W Murray. *Curr. Biol.***2005**, *15*, 1070-1076.
- [9] W D Gilliland, D L Vietti, N M Schweppe, F Guo, T J Johnson, R S Hawley. *PLoS ONE*.**2009**, *4*, e7544.
- [10] M Schmidt, Y Budirahardja, R Klompmaaker, R H Medema. *EMBO Reports*.**2005**, *6*, 866-872.
- [11] A M Wengner, G Siemeister, M Koppitz, V Schulze, D Kosemund, U Klar, D Stoeckigt, R Neuhaus, P Lienau, B Bader, S Prechtel, M Raschke, A -L Frisk, O von Ahsen, M Michels, B Kreft, F von Nussbaum, M Brands, D Mumberg, K Ziegelbauer. *Mol. Cancer Ther.***2016**.
- [12] RCSB, Protein Data Bank. <http://www.pdb.org/>. **2015**.
- [13] MOE, manual version 2015.09, Molecular Operating Environment (MOE), Chemical Computing Group, <http://www.chemcomp.com>, Montreal, Canada **2015**.
- [14] MOE, Molecular Operating Environment, Chemical Computing Group, <http://www.chemcomp.com>, Montreal, Canada. **2015**.
- [15] P Labute. *Journal of the Chemical Computing Group*. <http://www.chemcomp.com/journal/cstat.htm>., **2001**.
- [16] Timtec Ltd. www.timtec.net.
- [17] T A Halgren. *J. Comput. Chem.***1999**, *20*, 720-729.
- [18] T A Halgren. *J. Comput. Chem.***1996**, *17*, 616-641.
- [19] T A Halgren. *J. Comput. Chem.***1996**, *17*, 490-519.
- [20] T A Halgren. *J. Comput. Chem.***1996**, *17*, 553-586.
- [21] T A Halgren. *J. Comput. Chem.***1996**, *17*, 520-552.
- [22] T A Halgren, R B Nachbar. *J. Comput. Chem.***1996**, *17*, 587-615.
- [23] T A Halgren. *J. Comput. Chem.***1999**, *20*, 730-748.
- [24] M A Ghattas, N Atatreh, E V Bichenkova, R A Bryce. *J. Mol. Graph. Model.***2014**, *52*, 114-123.
- [25] NCI, National Cancer Institute. www.cancer.gov. 2015.
- [26] D F Veber, S R Johnson, H -Y Cheng, B R Smith, K W Ward, K D Kopple. *J. Med. Chem.***2002**, *45*, 2615-2623.
- [27] C A Lipinski, F Lombardo, B W Dominy, P J Feeney. *Adv. Drug Deliv. Rev.***1997**, *23*, 3-25.
- [28] MDL, MACCS Keys, MDL Information Systems Inc., 14600 Catalina Street, San Leandro, CA 94577. 2015.
- [29] K M Branson, B J Smith. *Aust. J. Chem.***2004**, *57*, 1029-1037

[30] E Perola. *Proteins: Struct. Funct. Bioinf.* **2006**, 64, 422-435.

[31] M A Ghattas, R A Mansour, N Atatreh, R A Bryce. *Chem. Biol. Drug Des.* **2015**, 87, 131-142.